Supporting information

Phosphate-assisted one-pot synthesis of zirconium-containing mesoporous silica with uniquely photodegradation ability for Rhodamine B

Jiu-Yang Yang, Chun-Ming Zheng, Yan-Qing Wang, Ming-Lin Guo

1 Characterization

The X-ray powder diffraction (XRD) was carried out on a MiniFlex 600 instrument (Japan) with Cu Ka radiation (λ= 1.5406 Å) at 40 kV and 15 mA.

The small-angle X-ray scattering (SAXS) was collected on Rigaku D/MAX 2400 diffractometer equipped with a CuKα X-ray source operating at 40 kV and 50 mA.

TEM images were observed by a Hitachi H-7650 transmission electron microscopy and operated at 100 kV. Samples were prepared by dispersing composite in ethanol and depositing it on a carbon-coated cupper grid.

X-ray fluorescence (XRF, Horiba XGT-1000WR) was used to determine the chemical compositions of ZrP-MS and Ag_3PO_4-MS.

Nitrogen sorption isotherms were obtained with a Quantachrome Nova volumetric adsorption analyzer at 77.3 K with samples outgassed at 150 °C for 12 h. Pore size distribution was calculated from the desorption isotherm using the BJH model and the BET surface area from the relative pressure of 0.057–0.346.

UV−visible diffuse reflectance spectra were recorded within the 190−800 nm wavelength range using a U-3010 spectrophotometer (Hitachi).

The photoluminescence and photoluminescence excitation were measured with a F-380 fluorescence spectrophotometer provided by Tianjin Gangdong Sci. & Tech. Development Co. Ltd. (China). The excitation source consisted of a 150 W Xe lamp.

2 Analysis

2.1 Pseudo-first order kinetic model

The Langmuir-Hinshelwood model is well established for photocatalysis when the concentration of pollutants is very low [1]. The relevant equations are listed as follows:

$$\mathrm{r} = -\frac{dC}{dt} = \frac{\kappa_r KC}{1+KC} \quad (1)$$

$$\ln\frac{C_0}{C} = kt \quad (2)$$

where r is the reaction rate, κ_r is the reaction rate constant, K is the adsorption coefficient, and C is the reactant concentration (eq 1). If C is very small, eq 2 is obtained. C_0 and C are the concentration of reactant at time 0 and t, respectively, and k is the apparent first order rate constant. The k value is obtained from the gradient of the graph of $\ln(C_0/C)$ versus time.

2.2 Terephthalic acid fluorescence probe

The terephthalic acid photoluminescence probing technique was adopted to detect hydroxyl radicals. 50mg ZrP-MS catalyst was added to 200 mL aqueous solution containing 0.01 mol/L NaOH and 3.0 mmol/L terephthalic acids. Prior to irradiation, the suspension was stirred in the dark for 20 min. 3 ml of the suspension was collected at predetermined time intervals. The suspension was centrifuged at 6000 rpm for 2 min.

3 Results

Transmission electron micrograph (TEM) image of Ag_3PO_4-MS in Fig. S1a revealed that the morphology of Ag_3PO_4-MS was sheets particles with thickness of ca. 100-200 nm and showed that it also had 2D-hexagonal ordering. No evident particles were observed in the nanopores of Ag_3PO_4-MS.

Fig. S1b displayed a typical type IV nitrogen sorption isotherm with an H1 hysteresis loop, which was the characteristic of mesostructure ordered from Ag_3PO_4-MS. The BET surface area was 287.5

m^2/g and the total pore volume at P/P_0=0.99 was 0.917 cm^3/g.

The small-angle X-ray scattering (SAXS) in Fig. S2a showed five resolved peaks which indicated ordered pores. Comparison of the structural details of Ag_3PO_4-MS with other p6mm-type mesoporous silica, Ag_3PO_4-MS was a structural analogue of SBA-15 and MSU-H. The *d*-spacing of Ag_3PO_4-MS of 11.03 nm corresponded to a unit cell parameter *a* = 12.7 nm. The wall thickness estimated at ca. 3.9 nm. Ag_3PO_4-MS had a mean pore diameter 8.8 nm according to BJH (see insert in Fig. S1b). The X-ray diffraction patterns (XRD) of Ag_3PO_4-MS (Fig. S2b) exhibited a broad and weak diffraction peak (2θ=15–30°), which could be attributed to amorphous silica composed of the composites. Other diffraction peaks of the composites could be easily indexed to the body-centered cubic structure of Ag_3PO_4 (JCPDS No. 06-0505). XRD pattern of Ag_3PO_4 is very sharp; this was not consistent with the Scherrer Formula prediction. But it was still not able to be explained. Maybe it was because Ag_3PO_4-MS were inhomogeneous materials.

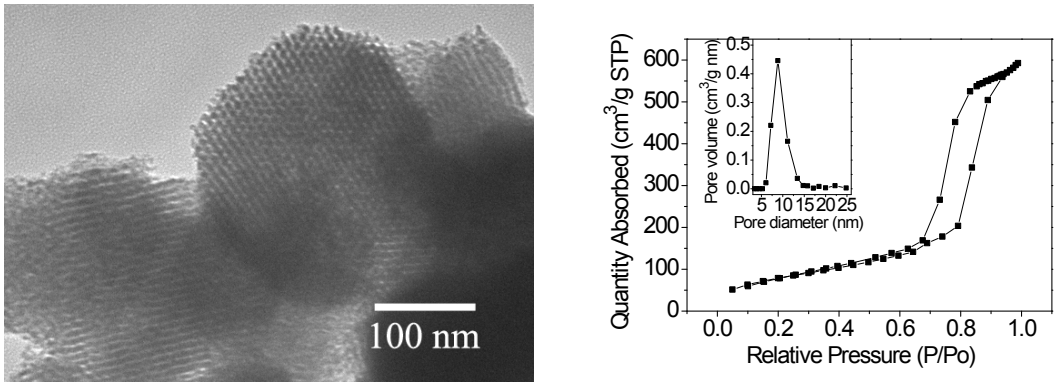

(a) (b)

Fig. S1 (a) TEM images of Ag_3PO_4-MS. (b) Nitrogen adsorption isotherm of Ag_3PO_4-MS. Inset: BJH pore size distribution derived from the desorption branch.

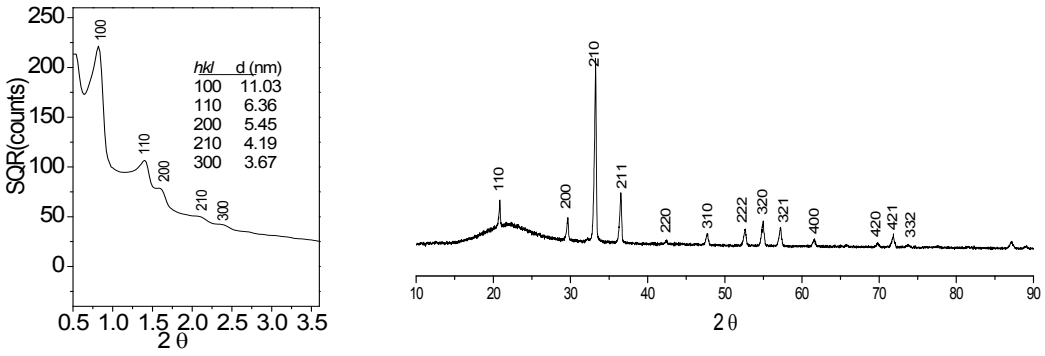

(a) (b)

Fig. S2 (a) SAXS pattern of Ag_3PO_4-MS. (b) The XRD of Ag_3PO_4-MS.

The Ag_3PO_4-MS was characterized by X-ray photoelectron spectroscopy (XPS) techniques. Two strong peaks at 531.20 and 102.17 eV were attributed to O_{1s} and Si_{2p}, in which the O/Si atomic ratio was 1.82, implying that the silicate walls in Ag_3PO_4-MS were highly condensed. Only 1.41 atom % of Ag_{3d} was found. The Ag_{3d} peaks were composed of two individual peaks (see Fig. S4) at 374.48 and 368.58 eV, which could be attributed to $Ag_{3d3/2}$ and $Ag_{3d5/2}$ binding energies, respectively [2], but no P_{2p} peaks were observed. XRF analysis showed that the element contents of silicon, silver and phosphors were 99.29 % in total, the Ag/P atomic ratio was determined as 3.90, suggesting the presence of some silver oxide or silver silicate species on the surface of the composites (see Table S2). Combined with the results of TEM, SAXS, XRD and nitrogen adsorption, most of Ag_3PO_4 in Ag_3PO_4-MS could be in tiny particles and dispersed in its silica walls. Silver phosphate was uniformly distributed in the silica.

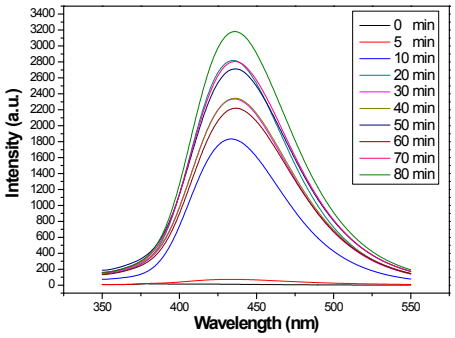

Fig. S3 The fluorescence spectra of the capture to hydroxyl radical for ZrP-MS system.

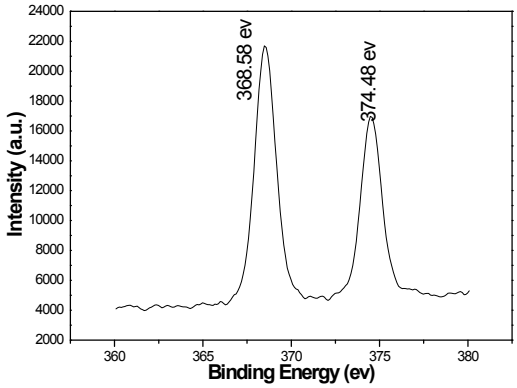

Fig. S4 XPS spectra of C 1s for Ag_3PO_4-MS (Ag3d)

Table S1 XRF analysis of ZrP-MS

Element	Average content %
Si	70.4017
Zr	20.7086
P	4.8922
Na	2.8134
Hf	0.579
Al	0.1856
S	0.0114
Cl	0.0695
Fe	0.1408
K	0.1191
Ca	0.0599
Ti	0.0029
Mo	0.0158

Table S2 XRF analysis of Ag_3PO_4-MS

Element	Average content %
Si	76.3179
Ag	21.3965
P	1.5745
Na	0.085
Mg	0.0109
Al	0.1568
S	0.1308
Cl	0.0938
Fe	0.2336

References

[1] V. A. Sakkas, I. M. Arabatzis, I. K. Konstantinou, A. D. Dimou, T. A. Albanis, P. Falaras, Appl. Catal. B, 2004, 49, 195-205.

[2] H. Zhang, G. Wang, D. Chen, X. Lv, J. Li, Chem. Mater., 2008, 20, 6543-6549.